Article

Effects of CuO Sintering Aids on Microstructure and Electric Properties for $(Na_{0.48}K_{0.473}Li_{0.04}Sr_{0.007})(Nb_{0.883}Ta_{0.05}Sb_{0.06}Ti_{0.007})O_3$ Ceramics

Cheng-Shong Hong *[ORCID], **Yuan-Xin Zhang and Yi-Tian Hong**

Department of Electronic Engineering, National Kaohsiung Normal University, Kaohsiung 82444, Taiwan; simon80428@gmail.com (Y.-X.Z.); soulkid4627@gmail.com (Y.-T.H.)
* Correspondence: cshong@nknu.edu.tw; Tel.: +886-7-7172930 (ext. 7915); Fax: +886-7-6051330

Abstract: In this paper, the effects of CuO sintering aids on microstructure and electric properties are investigated for the non-stoichiometric $(Na_{0.48}K_{0.473}Li_{0.04}Sr_{0.007})(Nb_{0.883}Ta_{0.05}Sb_{0.06}Ti_{0.007})O_3 + x$ mol% CuO lead free ceramics. As the amounts of CuO equal 1 mol%, the sintering temperature is 975 °C and the piezoelectric parameters are d_{33} = 200 pC/N, g_{33} = 38 (10^{-3} Vm/N), $d_{33} \times g_{33}$ = 7600 (10^{-15} m^2/N), k_p = 0.38, Q_m = 240, P_r = 18.93 μC/cm^2 and E_C = 8.75 kV/cm. The piezoelectric properties are changed to hard type and suitable for energy harvester with multilayer technology. The physical response mechanisms are suggested that the diffused phase transitions are enhanced, the Cu^{2+} ions substitute for the B-site ions with forming the Oxygen vacancies and the domain walls are pinning.

Keywords: lead-free; NKLNTS; CuO; dielectric; piezoelectric; pinning

1. Introduction

The piezoelectric effect has been widely used in various piezoelectric components, such as surface acoustic wave (SAW) filters, sensors, actuators, ultrasonic motors, transducers, speakers and energy harvesting. The National Bureau of Standards (NBS) reported the lead zirconate titanate PbTiO$_3$-PbZrO$_3$(PZT) as lead-based piezoelectric ceramics system in 1955 [1–4]. Because of the excellent piezoelectric behavior such as high surface phase velocity and electromechanical coupling coefficient, the PZT ceramics become the mainstream materials. However, there are a general awareness about environmental protection in recent year because of the Pb-based polluted materials [2–5]. European Union enforced the Restriction of the use of Hazardous Substance (RoHS) to restrict the heavy metal elements and their chemical compounds (Pb, Cd, Hg and so on) used at electrical and electronic engineering yields in 2006 [4]. Therefore, the development of lead-free piezoelectric materials is very important to replace lead zirconate titanate.

Nowadays, $(Ba_{1-x}Ca_xTi_{1-x}Zr_x)O_3$ (BCTZ) is the common lead free piezoelectric ceramic. However, the sinter temperature of BCTZ-based is too high (about 1450 °C) and have low Curie temperature (about 120 °C). In addition, the mainstream of lead-free piezoelectric materials includes $(Bi_{1-x}Na_x)TiO_3$ (BNT) and $(Na_{1-x}K_x)NbO_3$ (NKN) based materials. Although BNT materials have high tetragonal-cubic phase transition temperature (T_C ~600 °C) and high mechanical quality factor (Q_m ~7000), the electromechanical coupling coefficient k_p is very low (~22%) and the bismuth element is also poisonous [2]. Therefore, the NKN material is one of the most potential candidate material system. The pure NKN materials have high piezoelectric coefficient and high phase transition (T_C ~420 °C) [2–6]. However, since the Na and K atoms are volatile at the high sinter temperature (>800 °C), it is difficult to obtain the high density (4.25 g/cm^3) and high electromechanical coupling factor (k_p = 25~35%) NKN-based ceramics by using traditional sintering process [2–6]. Until now, researchers have developed many methods to overcome the problem of low density and easily deliquescence, such as: two step sintering, spark plasma sintering (SPS) and hot pressing [3–6]. However, these processes are too expensive and complex

to apply for the industrial fabrication. Therefore, researchers increase the bulk density of NKN-based materials by doping the ABO_3-types (A = Li, Sr; B = Sb, Ta) ferroelectrics and non-ferroelectrics [6–8]. With adding other ABO_3-type compounds, the orthorhombic-tetragonal phase transition temperature (T_{O-T}) effectively shift to room temperature and the soft piezoelectric properties are enhanced, such as (Na, K, Li)(Nb, Sb)O_3, (Na, K, Li)NbO_3, (Na, K, Li)(Nb, Ta)O_3 and (Na, K, Li)(Nb, Sb, Ta)O_3 [3,6,8,9]. Additionally, the addition of excess alkaline oxide can reduce the sintering temperature and compensate the evaporated alkali metal during the sintering process [9]. Moreover, the sintering aids like CuO, LiF, ZnO, Li_2CO_3, Bi_2O_3 and MnO_2 effectively decrease the sintering temperature for the NKN-based ceramics and improve the mechanical quality factor without reducing the piezoelectric properties [1–9]. Among them, the CuO sintering aids not only improve the grains growth and density for NKN-based ceramics but also Cu^{2+} ions which as an acceptor substitute for the B-site ions and create the oxygen vacancies for charge balance. This mechanism can increase the quality factor Q_m by preventing the movement of domain walls and the materials are changed to the hard piezoelectric properties [5–7,9]. Azough et al. [6] reported the $Na_{0.475}K_{0.475}Li_{0.05}NbO_3$ (NKLN) ceramics doped with CuO, the mechanical quality factor Q_m increase from 50 to 260 and the sintering temperatures reduce to below 900 °C because of the CuO sintering aids. Kim et al. [9] also reported the $(K_{0.485}Na_{0.515})_{0.935}Li_{0.065}](Nb_{0.99}Ta_{0.01})O_3$ (KNLNT) ceramics co-doped with the additions of CuO and Na_2CO_3, the sintering temperatures decrease from 1080 °C to 940 °C and the quality factors Q_m increase from 62 to 904.

Saito et al. [10] reported the NKN ceramics co-doped with $LiTaO_3$ and $LiSbO_3$, the $(K_{0.44}Na_{0.52}Li_{0.04})(Nb_{0.86}Ta_{0.10}Sb_{0.04})O_3$ ceramics have an excellent property compared with PZT ceramics system. Its piezoelectric constant d_{33} up to as high as 300 pC/N, which is far superior to the pure NKN (d_{33} = 190 pC/N) ceramics. Zhao et al. [8] suggested that the physical mechanism is polymorphic phase transition (PPT) like as morphotropic phase boundary (MPB) of Pb-based ceramics, which can improve piezoelectric behavior conspicuously. Zheng and Wang et al. [11] also reported that the (Na, K, Li)(Nb, Sb, Ta)O_3 (NKLNST) ceramics modified with Sr additives, the diffuseness of cubic-tetragonal phase transition is enhanced and the density and piezoelectric properties are improved. Su et al. [12] reported that the effects of $SrTiO_3$ dopants for the nonstoichiometric $(Na_{0.48-x}K_{0.48-x}Li_{0.04}Sr_x)Nb_{0.89-x}Ti_xTa_{0.05}Sb_{0.06}O_3$ ceramics, the dielectric loss *tanδ* is obviously reduced by the $SrTiO_3$ dopants. The excellent piezoelectric properties of d_{33} = 280 (pC/N), k_p = 0.47, ε = 1666, *tanδ* = 0.02, g_{33} = 19 (10^{-3} Vm/N), $d_{33} \times g_{33}$ = 5202 (10^{-15} m^2/N), P_r = 15.1 (μC/cm^2) and E_c = 14.2 (kV/cm) are obtained as x is 0.007 for the NKLNTS-ST ceramics. They suggested that the PPT regions (the phase coexistence of orthorhombic and tetragonal phases) exist between $0.005 \leq x \leq 0.008$ for $(Na_{0.48-x}K_{0.48-x}Li_{0.04}Sr_x)Nb_{0.89-x}Ti_xTa_{0.05}Sb_{0.06}O_3$ ceramics and lead to a significant improvement of the electric properties. By using the tape casting technology, the $(Na_{0.48}K_{0.473}Li_{0.04}Sr_{0.007})(Nb_{0.883}Ta_{0.05}Sb_{0.06}Ti_{0.007})O_3$ (NKLNTS-ST) ceramics were reported by Hong et al. [13]. The optimum sintering temperature is 1080 °C and the piezoelectric parameters are d_{33} = 288 pC/N, g_{33} = 20 (10^{-3} Vm/N), $d_{33} \times g_{33}$ = 5760 (10^{-15} m^2/N), k_p = 0.4, Q_m = 75. Although the NKLNTS-ST ceramics have good electrical properties for the tape casting technology, there are still some disadvantages. First, the sintering temperature is too high to obtain the multilayer components. Second, Na and K are easily volatile because of the high sintering temperature which causes the low density. Third, the quality factor Q_m and the piezoelectric parameter g_{33} are too low to applicate for energy harvester. Therefore, the CuO sintering aids are used to decrease the sintering temperature and improve the quality factor Q_m and the piezoelectric parameter g_{33}. This is the motivation of the present work.

Although the electric properties of tape casting ceramics are inferior to bulk ceramics, but the tape casting technology play an important role for the fabrication of the multi-layer, thinner film and textured ceramics. Furthermore for comparing the electric properties with pure NKLNTS-ST ceramics fabricated by the tape casting technology [13], the NKLNTS-ST

ceramics doped with the CuO sintering aids are also synthesized by using the tape casting method in this study. The effects of CuO sintering aids are also investigated by using the XRD patterns, SEM images and density. The dielectric properties are analyzed by using the Curie-Weiss law, and the piezoelectric properties are estimated by the resonant frequency method and ferroelectric hysteresis loops.

2. Experimental Procedures

The lead free ceramics of $(Na_{0.48}K_{0.473}Li_{0.04}Sr_{0.007})(Nb_{0.883}Ta_{0.05}Sb_{0.06}Ti_{0.007})O_3 + x$ mol % CuO (NKLNTS-ST-xCuO, x = 0, 0.5, 1.0, 1.5, 2.0 mol%) were prepared by the raw materials of Na_2CO_3, K_2CO_3, Nb_2O_5, Li_2CO_3, Sb_2O_3, Ta_2O_5, $SrCO_3$, TiO_2 and CuO powders (purity: >99%) by using the tape casting method. The powders were mixed according to the NKLNTS-ST ceramics and ball-milled together in a polyethylene jar using ethanol (99% purity) as the medium. The slurry was dried and calcined at 800 °C for 4 h. The different mole ratios of CuO powders were doped into the NKLNTS-ST calcined powders and ball-milled again. The slurries were dried and calcined one more time at 800 °C for 4 h. The calcined powders were ball-milled with a solvent (50 vol.% ethanol and 50 vol.% toluene) and dispersant for 24 h. Next, binder and plasticizer were added and then ball-milled again for 24 h. The slurry was tape-cast to a thickness of 30 μm green sheet on an aluminium foil by using a doctor blade apparatus. After drying, fifteen layer green sheets were laminated, and then hot-pressed at temperature of 60 °C and pressure of 80 MPa for 5 min to form a 0.5 mm thick green sheet. The laminated green sheets were heated at 600 °C for 10 h to remove organic substances before sintering. The samples were sintered in air at 1080 °C for x = 0~0.5 mol% CuO and at 975 °C for x = 1~2 mol% CuO for 6 h. Silver paste was fired on the surfaces at 750 °C for 20 min for the measurement of electrical properties. The samples were poled in silicon oil under a DC field of 3.0 kV/mm at 60 °C for 20 min. The piezoelectric properties were measured after the poling for 24 h.

The phase relations were analyzed by X-ray diffraction (XRD) with Cu Kα radiation (λ = 0.154 nm). The microstructure was observed by using scanning electron microscopy (HR-SEM, HITACHI SU8000, Hitachi, Tokyo, Japan). The densities were measured by using the Archimedes method. The dielectric constants (in the range of 25 to 500 °C at 1 MHz) and piezoelectric properties were measured by using a precision impedance analyser (4294A, HP, USA). The piezoelectric constant d_{33} was measured at room temperature by utilizing a static piezoelectric-constant testing meter (APC Cat. #90-2030). The *P-E* hysteresis loops were measured by using a ferroelectric tester at 1 Hz (Precision Premier II Ferroelectric Tester, Radiant Technology, Albuquerque, NM, USA).

3. Results and Discussions

3.1. XRD Patterns

Figure 1a shows the XRD diffraction patterns of NKLNTS-ST-xCuO ceramics measured at room temperature. In Figure 1a, the XRD patterns exhibit a pure perovskite structure for NKLNTS-ST-xCuO ceramics with different amounts of CuO sintering aids. Furthermore, there are no obvious second phase. The phenomenon is similar with the previous reports [14,15]. Kim et al. and Yin et al. suggested that the CuO additives dissolve into NKLNTS-ST and become a new solid solution [14,15]. In the previous report, researchers used the relative intensities peak of XRD patterns in 40~50° to investigate the phase structure for NKN-based ceramics [4–6,15–17]. In Figure 1b, the diffraction peaks of NKLNTS-ST-xCuO ceramics located at the range of 44~48° are all split with (220) and (002) peaks respectively. Wang et al. suggested that the split peaks show the phase coexistence of orthorhombic and tetragonal phases [18]. The phenomenon is called the polymorphic phase transition (PPT) and always helps to improve the piezoelectric performance [18]. Observing Figure 1b, the split (220) and (002) peaks are shifted to lower angle by increasing the amounts of CuO sintering aids. The results represent the lattice constants are increased by increasing the amounts of CuO sintering aids. Zhou et al. [19] reported that the Cu^{2+} ions play as an acceptor and enter into B site for NKN-based ceramics doping with CuO

additives. Yang et al. [2] also observed the lattices of NKN are increased with increasing the amounts of $CuNb_2O_6$ dopants for NKN ceramics doping with $CuNb_2O_6$ dopants. They suggested that the Cu^{2+} ions may substitute for both A and B sites and cause the lattice expansion. In addition, Li et al. [20] suggested that the Cu^{2+} ions enter into the A site as low amounts of CuO dopants and enter into the B site as high amounts of CuO dopants for NKN-based ceramics doping with CuO dopants. In conclusion, the response mechanisms are suggested that the Cu^{2+} ions enter into the A site of Na^+, K^+ and Li^+ ions initially as the few amounts of Cu^{2+} ions because the high volatilization of Na^+ and K^+ ions (about 800 °C) during sintering process. When the amounts of CuO sintering aids are increased, the more Cu^{2+} ions replace B-site with forming Oxygen vacancies for charge balance since the ionic radius of Cu^{2+} (0.73 Å) is similar and larger than B-site ions (Nb^{5+} = 0.64 Å, Ta^{5+} = 0.64 Å, Sb^+ = 0.61 Å and Ti^{2+} = 0.60 Å) [16,17].
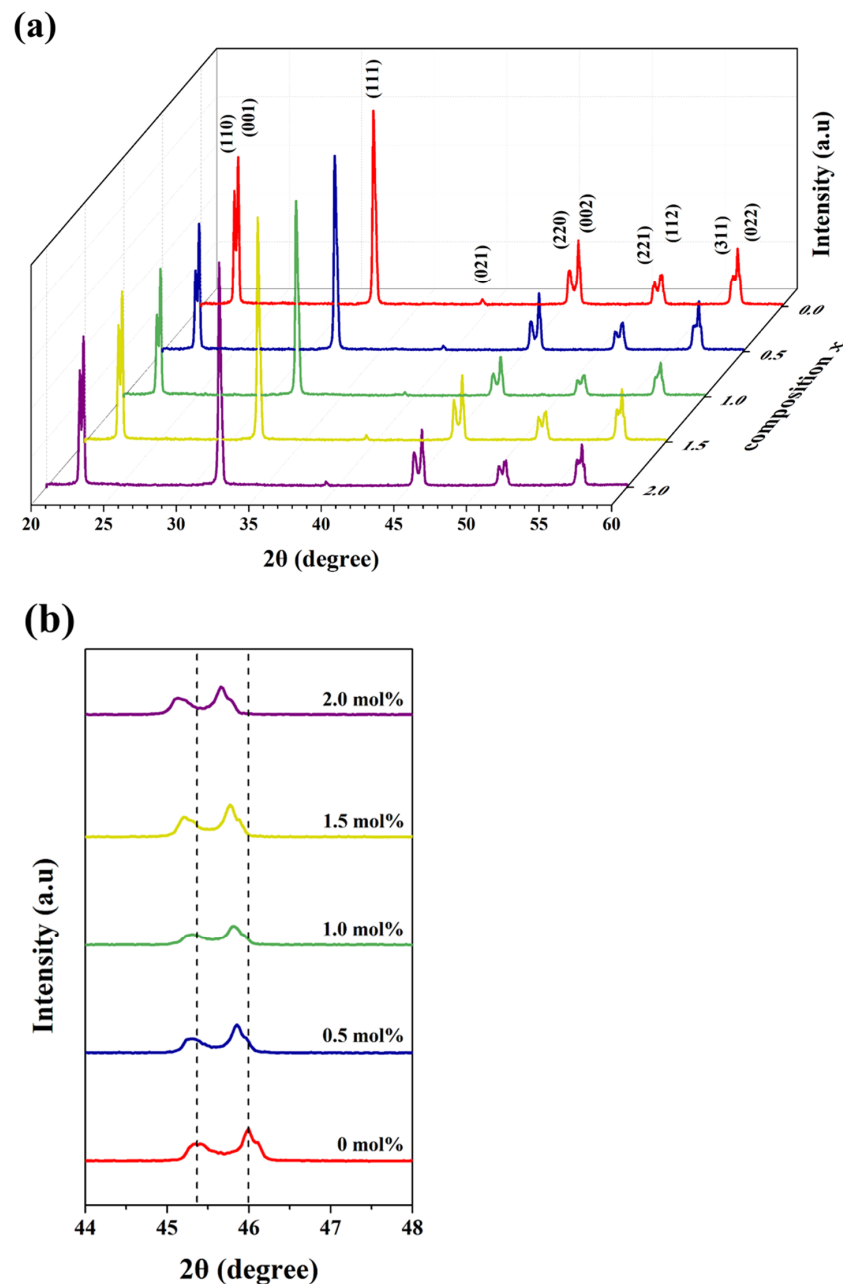
Figure 1. XRD diffraction patterns of NKLNTS-ST-*x*CuO ceramics at room temperature in the 2θ range of (**a**) 20~60° (**b**) 44~48°.

3.2. SEM Images and Densities

Figure 2 shows the SEM images of the NKLNTS-ST-xCuO (x = 0~2.0 mole%) ceramics. In Figure 2a, the grains display rectangle shape, the distribution of grain size ranges from 0.5 to 2.5 μm, the average size is 1.25 μm and few pores are observed. When the amounts of CuO sintering aids are increased as shown in Figure 2b–e, the average grain sizes are increased from 1.25 μm as x = 0 mole% to 3.42 μm as x = 2.0 mole%. The results are similar to the previous papers [4,5,16,19,21]. Lee et al. [4] reported that the CuO sintering aids can promote the grain growth for NKN ceramics doped with CuO additives and the response mechanism are suggested that the Cu^{2+} ions substitute for the B-site ions with the oxygen vacancies for charge balance. Weng et al. [5] also reported that the liquid phase enhance the grain growth by low melting point of Cu additives for NKN ceramics doped with CuF_2 dopants. Observing Figure 2b–e, the small grains and large grains are coexisting, and the large grains are increased with increasing the amounts of CuO sintering aids. The results are similar to the previous reports [2–5,19–23]. Zhou et al. and Zhao et al. [19] reported that the irregular and large grains are caused by the formation of the inhomogeneous distribution of liquid phase [22]. In addition, Lee et al. and Weng et al. reported that the secondary products ($K_4CuNb_8O_{23}$, $K_{5.4}Cu_{1.3}Sb_{10}O_{29}$ and $K_{5.4}Cu_{1.3}Ta_{10}O_{29}$) can be formed by excess B-site compositions (Nb, Sb and Ta) reacted with CuO when the B-site mol ratios are bigger than A-site mol ratios which caused by evaporating of Na^+ and K^+ ions [4,5]. According to our experimental data shown in Figures 1 and 2, the SEM images show the irregular and large grains and the XRD patterns don't show obvious second phase and lattice expansion. Therefore, the response mechanisms are suggested that the CuO maybe alone or forming the second product with the liquid phase to promote the grain growth. At last, the Cu^{2+} ions dissolve into the A-site vacancies caused by evaporation of Na^+ and K^+ ions as few amounts of CuO additives and substitute for the B-site with oxygen vacancies for charge balance as more amounts of CuO additives.

According to the previous reports, the electric properties of NKN-based ceramics are always not good because of more pores, less densities and nonhomogeneous structure since the Na^+ and K^+ ions are easily evaporated at high sintering temperature [5,17,24]. Table 1 shows the densities of NKLNTS-ST-xCuO ceramics with different amounts of CuO additives and the sintering temperatures are 1080 °C for x = 0~0.5 mol% and 975 °C for x = 1~2 mol%. In Table 1, the densities are continuously increased with increasing the amounts of CuO additives until x = 1 mol% and then the densities are decreased when the amounts of CuO additives are increased again. Furthermore, the sintering temperatures are obviously decreased from 1080 °C to 975 °C. The results are similar to the previous reports [4,5,23,25,26]. According to the discussions of SEM images and XRD patterns, the grain size and the lattice expansion are increased with increasing the amounts of CuO additives. In conclusion, the densities are increased with increasing the amounts of CuO additives since the grain size are increased and the pores between grain and grain are decreased when the amounts of CuO additives are low than 1 mol%. When the amounts of CuO additives are large than 1 mol%, the densities are decreased with increasing the amounts of CuO additives since the grain sizes are too large to induce the pores between grain and grain, the lattice expansions are enhanced and the pairs of Cu^{2+} ions and Oxygen vacancies are increased.

Table 1. Densities of NKLNTS-ST-xCuO ceramics.

	0 mol%	0.5 mol%	1.0 mol%	1.5 mol%	2.0 mol%
Density (g/cm^3)	4.64	4.72	4.75	4.68	4.65
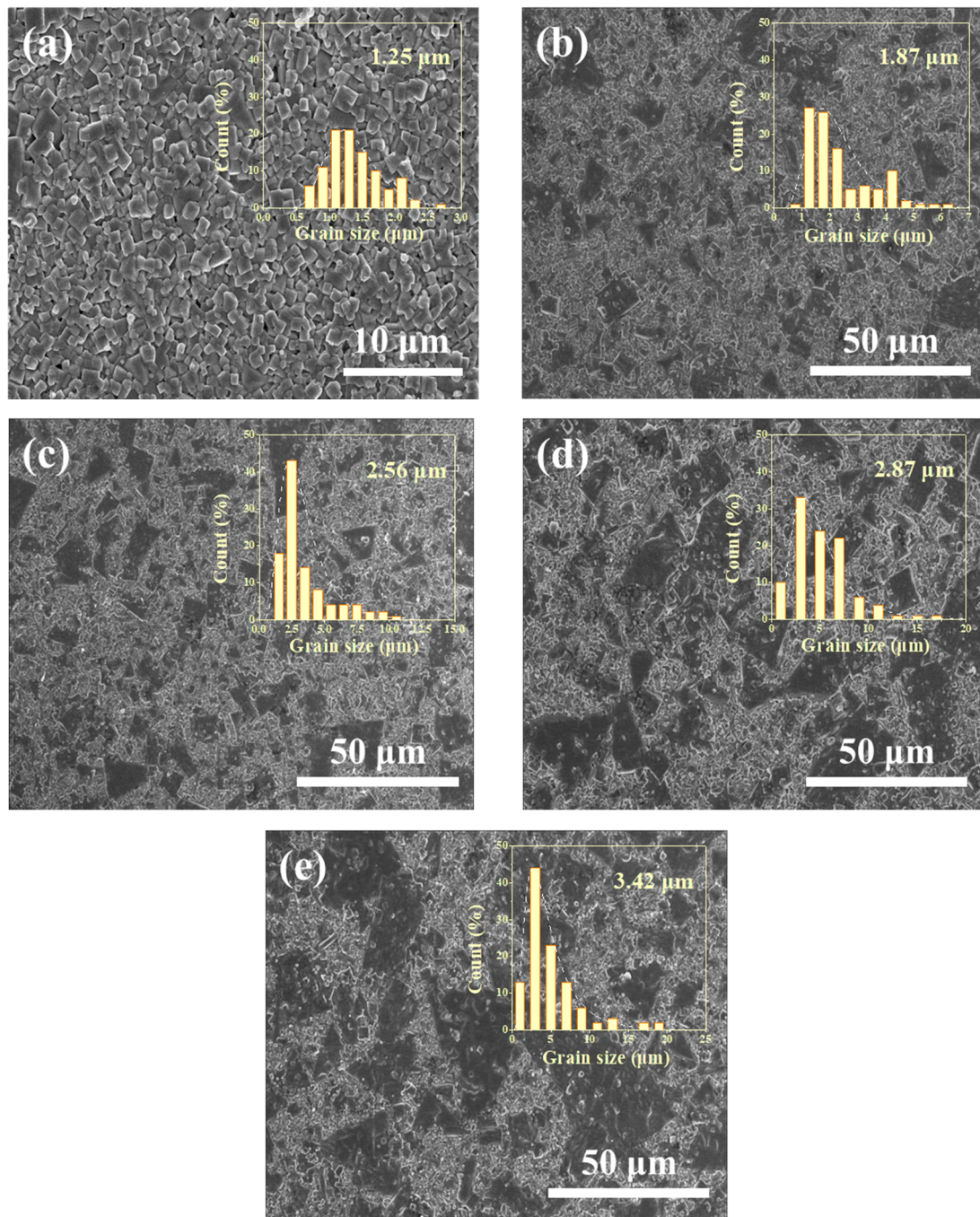
Figure 2. SEM images of the NKLNTS-ST-xCuO ceramics doped with (**a**) x = 0 mol%, (**b**) x = 0.5 mol%, (**c**) x = 1.0 mol%, (**d**) x = 1.5 mol% and (**e**) x = 2.0 mol%.

3.3. Dielectric Properties

Figure 3 shows the dielectric constants as a function of temperature measured at 100 kHz for NKLNTS-ST-xCuO (x = 0~2.0 mol%) ceramics. The NKLNTS-ST-xCuO ceramics have two phase temperatures close to 100~150 °C and 300~400 °C corresponding to the orthorhombic-tetragonal phase transition T_{O-T} and the tetragonal-cubic phase transition T_C, respectively. Both the T_{O-T} and T_C phase transition temperatures are decreased with increasing the CuO contents shown in Figure 4. This result is similar to the ceramics of the formula $K_{0.5}Na_{0.5}NbO_3$-x%CuO and $(K_{0.5}Na_{0.5})(Nb_{1-2x/5}Cu_x)O_3$ reported by Lin et al. and Tan et al. [27,28]. This is also an evidence like as the discussions of XRD patterns and

SEM images, the Cu^{2+} ions dissolve into the A-site or B-site and then change the lattice symmetry and the phase transition temperature [5,29]. In Figure 3, the peak dielectric constants corresponding to the phase transition are decreased and the dielectric peaks seem broader when the amounts of CuO additives are increased. The broad dielectric peaks always show more diffused phase transition behavior and relate to the Curie-Weiss law [30–32]. The Curie-Weiss law is usually used to describe the dielectric behaviour. As the temperature far above the Curie temperature T_C, the dielectric behavior obeys the Curie-Weiss law. The Curie–Weiss law shows as below [33]:

$$\chi = \frac{C}{T - \theta} \tag{1}$$

where χ is the dielectric susceptibility, *C* is the Curie-Weiss constant, and θ is the Curie-Weiss temperature, slightly lower than the phase transition temperature T_m corresponding to the maximum dielectric constant. Figure 5 shows the reciprocal dielectric susceptibilities as a function of temperature and the fitting curves according to the Curie-Weiss law for the NKLNTS-ST ceramic with 0 mol% CuO additive measured at 100 kHz. The dielectric behavior follows the Curie-Weiss law in the paraelectric region at enough high temperature, but it deviates from the Curie-Weiss law at lower temperatures (but still above T_m). T_B is the temperature at which the deviation begins, and the local order polarization is induced [30]. The correlation of neighboring polarization microregions induces the deviation from the Curie–Weiss law [31]. The empirical parameter ΔT_m is usually used to estimate the degree of deviation from the Curie-Weiss law [32,34]:

$$\Delta T_m = T_B - T_m \tag{2}$$
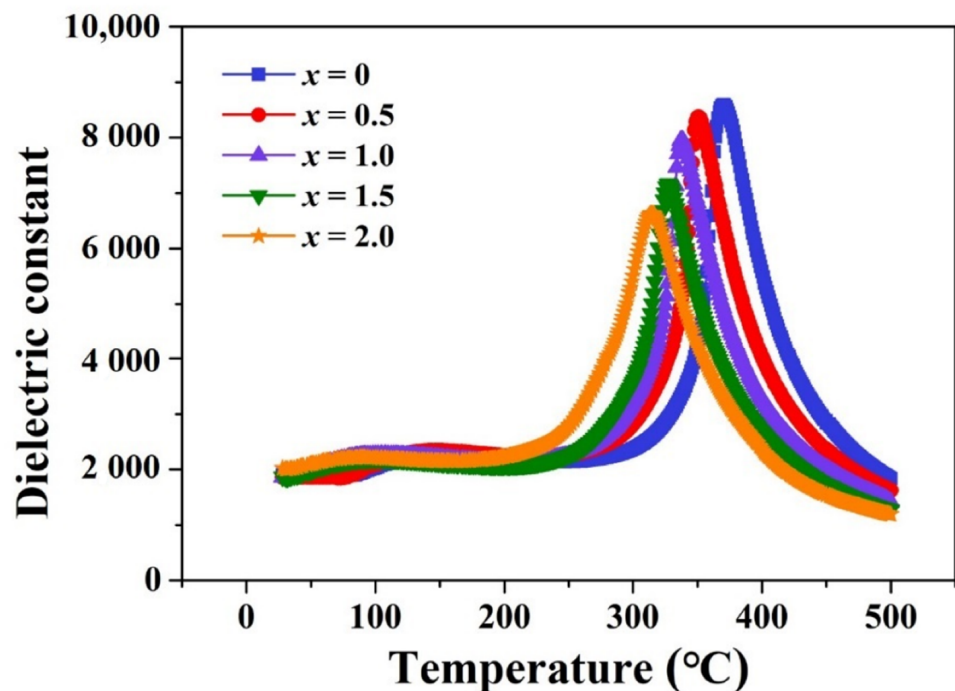
Figure 3. Temperature dependence of the dielectric constants for NKLNTS-ST-*x*CuO (*x* = 0~2.0 mol%) ceramics measured at 100 kHz.
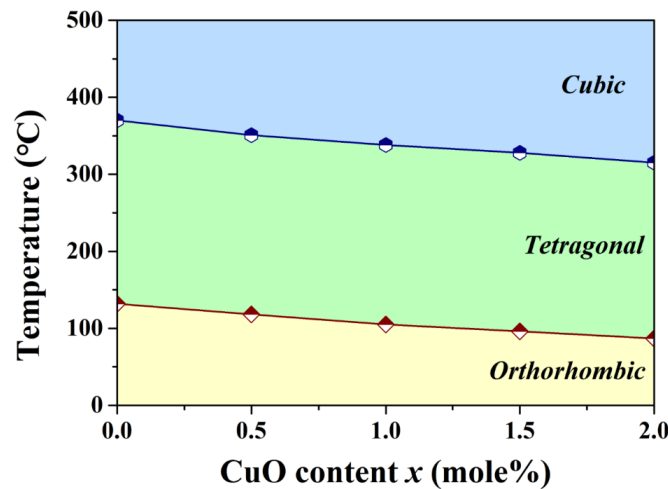
Figure 4. Variation of the phase transition temperatures for NKLNTS-ST-*x*CuO ceramics measured at 100 kHz.
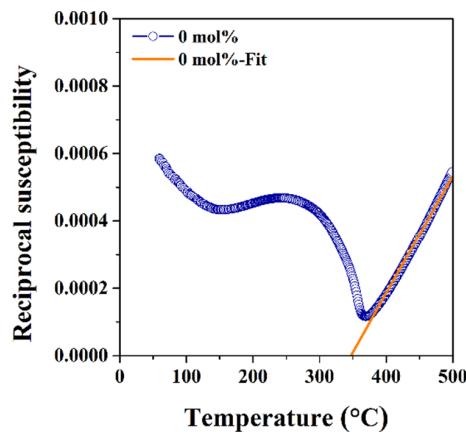

Figure 5. Temperature dependence of the reciprocal dielectric constants and fitting curves by using the Curie-Weiss law for NKLNTS-ST ceramic with 0 mol % CuO additive measured at 100 kHz.

According to Equationns (1) and (2), Figures 3 and 5, Table 2 shows the values of ΔT_m, T_B and T_m for NKLNTS-ST-*x*CuO ceramics. In Table 2, the ΔT_m values increase with increasing the amounts of CuO additives. The results represent that the dielectric behavior of NKLNTS-ST-*x*CuO ceramics exhibit more diffused phase transition behavior as increasing the amounts of CuO additives. According to the discussions of XRD patterns, SEM images and densities, the response mechanism is suggested that the Cu^{2+} ions dissolve into the A-site and B-site and then promote more ion or oxygen vacancies, more compositional fluctuation and more local distortion [35].

Table 2. Empirical parameters of the of NKLNTS-ST-*x*CuO ceramics.

Compositions (*x*)	0 mol%	0.5 mol%	1.0 mol%	1.5 mol%	2.0 mol%
T_B	387	386	383	374	362
T_m	352	346	338	325	300
ΔT_m	35	40	45	49	62

3.4. Piezoelectric Properties

Figure 6a shows the polarization-electric-field (*P-E*) hysteresis loops of the NKLNTS-ST-*x*CuO ceramics measured at a frequency of 1 Hz and room temperature. The ferroelectric hysteresis loops are obviously changed with increasing the amounts of CuO additives. The

P-E loop is skew to the horizontal axis with non-doped CuO additives, this means that the ferroelectric property has lower remnant polarization P_r and relative higher coercive electric field E_c. When the amounts of CuO additives are increased, the skew phenomena are decreased until 1 mol% CuO additives and then are enhanced again as high enough content of CuO additives. Furthermore, the double hysteresis loop is seemed as 2 mol% CuO additives. The results are similar to the previous reports [5,6,14,15,20,21,27,29]. For detailing the *P-E* hysteresis loops, the remnant polarizations P_r and coercive electric fields E_c are showed in Figure 6b. According to the previous reports and our experimental results, the response mechanisms are supposed as: (1) The more Cu^{2+} ions substitute for the A-site vacancies caused by evaporation of Na^+ and K^+ ions as few amounts of CuO additives and then the oxygen vacancies for neutrality of the evaporation of Na^+ and K^+ ions are decreased [5,6,20,21]. Therefore, the E_c values are decreased shown in Figure 6b since the pinning domain walls are decreased with decreasing the oxygen vacancies when the amounts of CuO additives are increased until 1 mol% CuO additives. (2) When the amounts of CuO additives are high than 1 mol%, the more Cu^{2+} ions enter into the B-site and induce the new oxygen vacancies for charge balance. Therefore, the E_c values are contrary increased with increasing the amounts of CuO additives shown in Figure 6b since the pinning domain walls are increased by the new oxygen vacancies [5,6,20,21]. (3) The double hysteresis loop is seemed as 2 mol% CuO additives shown in Figure 6a since the polarizations are insufficient time for the migration of Cu^{2+} ions and oxygen vacancies under the external field. Therefore, the defect dipoles stay at the original direction and provide a force to reverse the polarization switching as removing the external electric field. It also ascribes the pinning effects with hard piezoelectric properties because of the pairs of Cu^{2+} ions and oxygen vacancies [5,14,27,29]. (4) When the amounts of CuO additives are increased, the values of remnant polarizations P_r are increased until 1 mol% CuO additives shown in Figure 6b because of the more diffused phase transitions with abnormal dielectric behavior and the more densification as mention in Section 3.3 and 3.2. (5) When the amounts of CuO additives are high than 1 mol%, the P_r values are contrary decreased with increasing the amounts of CuO additives shown in Figure 6b because of the less densification as mentioned in Section 3.2 and the more pinning effect by the pairs of Cu^{2+} ions and oxygen vacancies [5,6,20,21]. In conclusion, the maximum remnant polarization P_r = 18.93 μC/cm² and minimum coercive electric field E_C = 8.75 kV/cm are obtained with a good piezoelectricity at 1 mol% CuO additives since there are the largest spontaneous polarizations and easily rotated under poling processing [36,37].
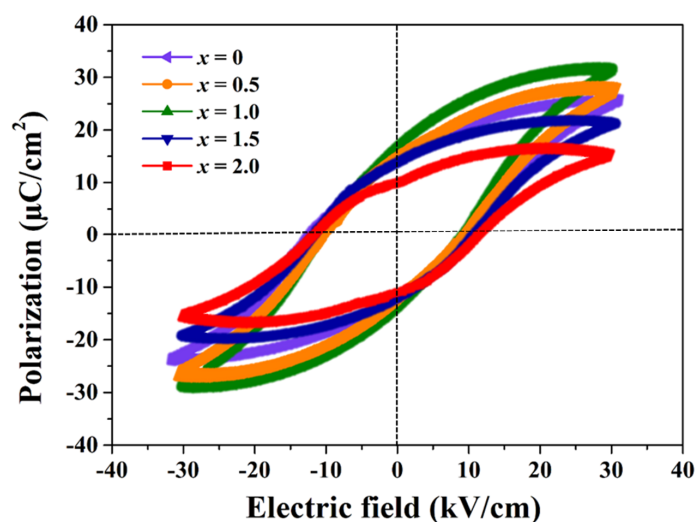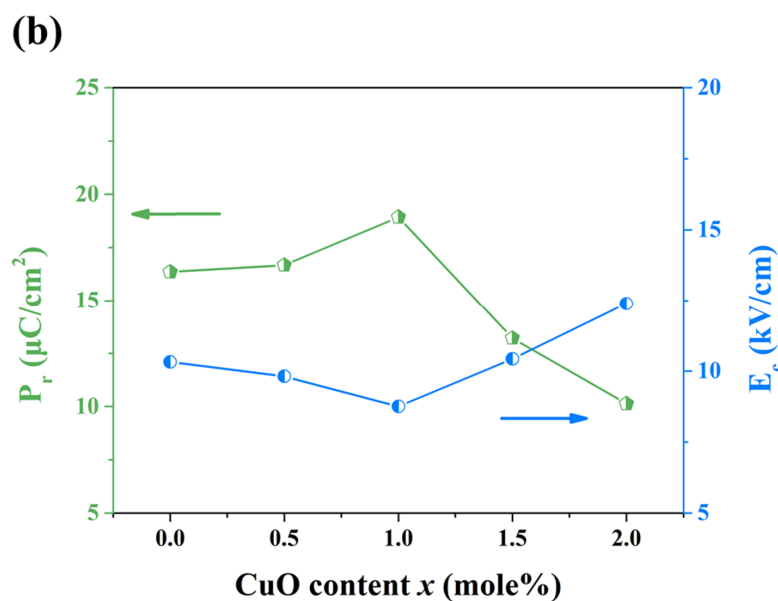
(a)

Figure 6. *Cont.*

(b)

Figure 6. (**a**) Ferroelectric hysteresis loop (*P-E* loop) and (**b**) Remnant polarization P_r and coercive electric field E_C of the NKLNTS-ST-xCuO ceramics measured at 1 Hz and room temperature.

Figure 7 shows the piezoelectric properties (k_p, Q_m, d_{33} and g_{33}) of the NKLNTS-ST-xCuO ceramics. In Figure 7, the values of k_p, d_{33} are decreased and the values of Q_m, g_{33} are increased when the amounts of CuO additives are increased. The results are similar the previous reports [5,6,14,15,20,21,27,29]. According to the experimental results and the previous reports, the response mechanisms are supposed as: (1) The values of k_p and d_{33} are decreased with increasing the amounts of CuO additives since the diffused phase dielectric behavior are enhanced as mentioned in Section 3.3 and the pinning effects of domain walls are increased by the pairs of Cu^{2+} ions and oxygen vacancies. (2) The values of Q_m are increased with increasing the amounts of CuO additives since the densities are increased as mentioned in Section 3.2 due to the liquid phase sintering in the range of 0~1 mol% CuO additives and the pinning effects of domain walls are enhanced by the pairs of Cu^{2+} ions and oxygen vacancies in the range of 1~2 mol% CuO additives. (3) The values of g_{33} are increased with increasing the amounts of CuO additives since the diffused phase transition with abnormal dielectric behavior are enhanced and the densities are increased in the range of 0~1 mol% CuO additives. In conclusion, the maximum spontaneous polarization, the minimum coercive electric field, the largest density, the optimum diffused phase dielectric behavior and the optimum pinning effects are obtained as 1 mol% CuO additives and the appropriate piezoelectric properties are obtained with d_{33} = 200 pC/N, g_{33} = 38 (10^{-3} Vm/N), $d_{33} \times g_{33}$ = 7600 (10^{-15} m^2/N), k_p = 0.38, Q_m = 240, P_r = 18.93 μC/cm^2 and E_C = 8.75 kV/cm. To compare the results of this work with the results of previous reports [4,6,7,9,13–16,19,20,22,23,27–29], Table 3 shows the comparing results. In Table 3, our sample has lower sintering temperature and higher piezoelectric coefficients of d_{33} and g_{33}. Some previous reports [4,7,9,14,23,27–29] seem have higher quality factor Q_m, but their piezoelectric coefficients are far lower than our sample. Specially, our samples are synthesized by the tape casting technology and other reports are synthesized by the conventional method with uniaxial pressed process. Generally, the sample synthesized by the tape casting technology have lower density. Comparing the results of reference 13 with our sample, our sample have lower sintering temperature, higher piezoelectric coefficients $d_{33} \times g_{33}$ and higher quality factor Q_m. Comparing the results of reference 22 with our sample, the sintering temperature, piezoelectric coefficients d_{33} and quality factor Q_m are small better than our sample. However, our sample are synthesized by the tape casting technology suitable for multilayer devices.
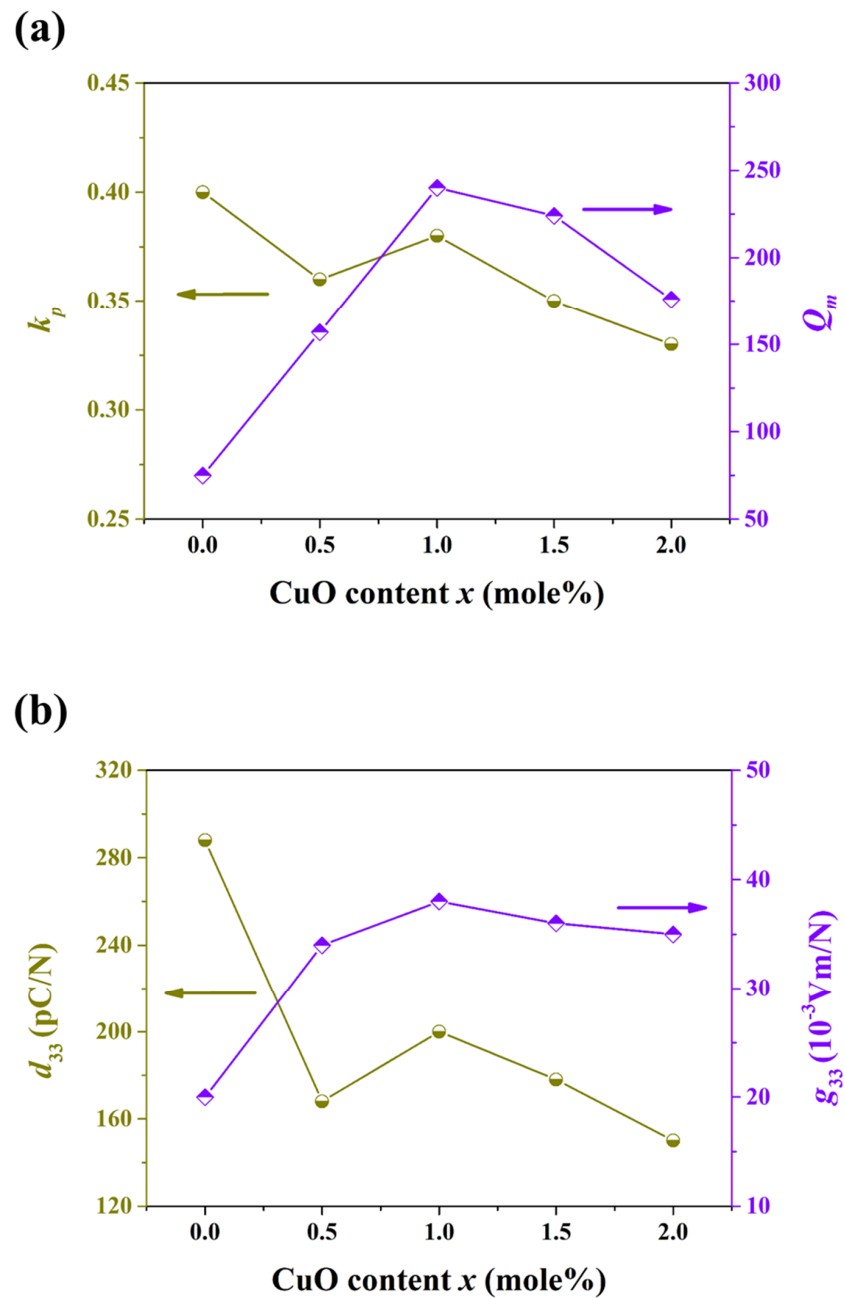
(a)

(b)

Figure 7. Piezoelectric parameters (**a**) k_p, Q_m and (**b**) d_{33}, g_{33} of NKLNTS-ST-xCuO ceramics.

Table 3. Comparison of this work with the previous reports.

Composition	Synthesis	Sintering	d_{33}	g_{33}	Q_m	Reference
NKLNTS-ST + CuO	T	975	200	38	240	This work
NKNS + CuO + Ag$_2$O	C	1080	70	-	540	[4]
NKLN + CuO	C	1100	285	-	220	[6]
NKCN + CuO	C	1080	-	39	2850	[7]
NKLNT + CuO + Na$_2$CO$_3$	C	940	145	-	904	[9]
NKLNTS-ST	T	1080	288	20	75	[13]
CKN	C	960	80	-	3005	[14]
NKN-LN + CuO	C	950	173	-	207	[15]
NKLNS-CZ + CuO	C	1100	238	-	-	[16]
NKLNT-AS + CuO	C	970	383	-	188	[19]
NKLNTS + CuO	C	1165	64	-	137	[20]

Composition	Synthesis	Sintering	d_{33}	g_{33}	Q_m	Reference
NKN-LNS + CuO	C	960	207	-	320	[22]
NKN + CuO	C	1100	95	-	2100	[23]
NKN + CuO	C	1120	82	-	2523	[27]
KNNC	C	1070	90	-	1241	[28]
KNN + CuO	C	1090	82	-	2525	[29]

Synthesis method: T (tape casting), C (conventional uniaxial pressed process). Unit: Sintering (°C), d_{33} (pC/N), g_{33} (10^{-3} Vm/N).

4. Conclusions

In this paper, the effects of CuO sintering aids are investigated for the non-stoichiometric NKLNTS-ST-*x*CuO lead free ceramics. The lattice structure, microstructure and electrical properties are investigated by the XRD patterns, SEM images, Curie-Weiss law and domain walls pinning effect. The sintering temperatures are decreased from 1080 °C to 975 °C because of the liquid phase sintering. Furthermore, the optimum piezoelectric properties are changed from soft type to hard type due to the CuO sintering aids and the domain walls pinning effect. Especially, the piezoelectric parameters are $d_{33} = 288$ pC/N, $g_{33} = 20$ (10^{-3} Vm/N), $k_p = 0.4$, $Q_m = 75$, $d_{33} \times g_{33} = 5760$ (10^{-15} m^2/N) for pure NKLNTS-ST ceramics and the piezoelectric parameters are $d_{33} = 200$ pC/N, $g_{33} = 38$ (10^{-3} Vm/N), $k_p = 0.38$, $Q_m = 240$, $d_{33} \times g_{33} = 7600$ (10^{-15} m^2/N) for NKLNTS-ST-1 mol% CuO ceramics. In conclusion, the NKLNTS-ST-*x*CuO ceramics are suitable for energy harvester and multilayer fabricating processes using Ni electrodes since the sintering temperatures are decreased from 1080 °C to 975 °C, the quality factors Q_m are increased from 75 to 240 and the piezoelectric parameters $d_{33} \times g_{33}$ are increased from 5760 (10^{-15} m^2/N) to 7600 (10^{-15} m^2/N).

Author Contributions: Conceptualization, C.-S.H. and Y.-T.H.; supervision, C.-S.H.; data curation, Y.-T.H.; writing—original draft preparation, C.-S.H. and Y.-X.Z.; writing—review and editing, C.-S.H. and Y.-X.Z. All authors contributed equally to this work. All authors have read and agreed to the published version of the manuscript.

Institutional Review Board Statement: Not applicable.

Informed Consent Statement: Not applicable.

Data Availability Statement: The data that supports the findings of this study are available within the article.

Conflicts of Interest: The authors declare no conflict of interest.

References

1. Jaffe, B.; Cook, W.R.; Jaffe, H.L. *Piezoelectric Ceramics*; Academic Press: New York, NY, USA, 1971.
2. Yang, M.R.; Chu, S.Y.; Tsai, C.C. An ultrasonic therapeutic transducers using lead-free Na$_{0.5}$K$_{0.5}$NbO$_3$-CuNb$_2$O$_6$ ceramics. *J. Alloys Compd.* **2010**, *507*, 433–438. [CrossRef]
3. Rani, R.; Sharma, S.; Rai, R.; Kholkin, A.L. Dielectric behavior and impedance analysis of lead-free CuO doped (Na$_{0.50}$K$_{0.50}$)$_{0.95}$ (Li$_{0.05}$Sb$_{0.05}$Nb$_{0.95}$)O$_3$ ceramics. *Solid State Sci.* **2013**, *17*, 46–53. [CrossRef]
4. Lee, Y.; Yoo, J.; Lee, K.; Kim, I.; Song, J.; Park, Y.W. Dielectric and piezoelectric characteristics of the non-stoichiometric (Na, K)NbO$_3$ ceramics doped with CuO. *J. Alloys Compd.* **2010**, *506*, 872–876. [CrossRef]
5. Weng, C.M.; Tsai, C.C.; Sheen, J.; Hong, C.S.; Chu, S.Y.; Chen, Z.Y.; Su, H.H. Low-temperature-sintered CuF$_2$-doped NKN ceramics with excellent piezoelectric and dielectric properties. *J. Alloys Compd.* **2017**, *698*, 1028–1037. [CrossRef]
6. Azough, F.; Wegrzyn, M.; Freer, R.; Sharma, S.; Hall, D. Microstructure and piezoelectric properties of CuO added (K, Na, Li)NbO$_3$ lead-free piezoelectric ceramics. *J. Eur. Ceram. Soc.* **2011**, *31*, 569–576. [CrossRef]
7. Tsai, C.C.; Chu, S.Y.; Hong, C.S.; Yang, S.L. Influence of A-site deficiency on oxygen-vacancy-related dielectric relaxation, electrical and temperature stability properties of CuO-doped NKN-based piezoelectric ceramics. *Ceram. Int.* **2013**, *39*, S165–S170. [CrossRef]

8.   Zhao, X.; Zhang, B.; Zhu, L.; Zhao, L.; Zhou, P. Study of polymorphic phase boundary in (Na, K, Li)(Nb, Ta, Sb)O$_3$ piezoelectric ceramics. *J. Phys. D Appl. Phys.* **2014**, *47*, 065105. [CrossRef]

9.   Kim, J.; Kim, J.; Han, S.; Kang, H.W.; Lee, H.G.; Cheon, C. Low-temperature sintering and piezoelectric properties of CuO-doped (K,Na)NbO$_3$ ceramics. *Mater. Res. Bull.* **2017**, *96*, 121–125. [CrossRef]

10. Saito, Y.; Takao, H.; Tani, T.; Nonoyama, T.; Takatori, K.; Homma, T.; Nagaya, T.; Nakamura, M. Lead-free piezoceramics. *Nature* **2004**, *432*, 84–87. [CrossRef]

11. Zheng, L.; Wang, J.; Ming, B.; Wang, C.; Du, J.; Wu, Q. Phase structure and electrical properties of strontium modified (Na$_{0.48-x}$K$_{0.48-x}$Li$_{0.04}$Sr$_x$)Nb$_{0.89}$Ta$_{0.05}$Sb$_{0.06}$O$_3$ ceramics. *Phys. Status Solidi A* **2009**, *206*, 1602–1605. [CrossRef]

12. Su, H.H.; Hong, C.S.; Tsai, C.C.; Chu, S.Y. Electric properties of SrTiO$_3$ modified (Na$_{0.48}$K$_{0.48}$Li$_{0.04}$)Nb$_{0.89}$Ta$_{0.05}$Sb$_{0.06}$O$_3$ lead-free ceramics. *ECS J. Solid State Sci. Technol.* **2016**, *5*, N67. [CrossRef]

13. Hong, C.S.; Hong, Y.T. Effects of sintering temperature on structure and electrical properties of (Na$_{0.48}$K$_{0.473}$Li$_{0.04}$Sr$_{0.007}$) (Nb$_{0.883}$Ta$_{0.05}$Sb$_{0.06}$Ti$_{0.007}$)O$_3$ piezoelectric ceramics. *Process. Appl. Ceram.* **2021**, *15*, 79–86. [CrossRef]

14. Kim, J.H.; Kim, D.H.; Seo, I.T.; Hur, J.; Lee, J.H.; Kim, B.Y.; Nahm, S. Effect of CuO on the ferroelectric and piezoelectric properties of lead-free KNbO$_3$ ceramics. *Sens. Actuator A Phys.* **2015**, *234*, 9–16. [CrossRef]

15. Yin, Q.; Yuan, S.; Dong, Q.; Tian, C. Effect of CuO and MnO$_2$ doping on electrical properties of 0.92(K$_{0.48}$Na$_{0.54}$)NbO$_3$-0.08LiNbO$_3$ under low-temperature sintering. *J. Alloys Compd.* **2010**, *491*, 340–343. [CrossRef]

16. Zhang, Y.; Li, M.; Li, H.; Zhai, J. Effects of CuO on KNN-based ceramics. *Inorg. Chem. Commun.* **2020**, *122*, 108299. [CrossRef]

17. Yang, S.L.; Tsai, C.C.; Hong, C.S.; Chu, S.Y. Effects of sintering aid CuTa$_2$O$_6$ on piezoelectric and dielectric properties of sodium potassium niobate ceramics. *Mater. Res. Bull.* **2012**, *47*, 998–1003. [CrossRef]

18. Wang, K.; Li, J.F. Domain engineering of lead-free Li-modified (K,Na)NbO$_3$ polycrystals with highly enhanced piezoelectricity. *Adv. Funct. Mater.* **2010**, *20*, 1924–1929. [CrossRef]

19. Zhou, J.J.; Cheng, L.Q.; Wang, K.; Zhang, X.W.; Li, J.F.; Liu, H.; Fang, J.Z. The phase structure and electric properties of low-temperature sintered (K,Na)NbO$_3$-based piezoceramics modified by CuO. *Ceram. Int.* **2014**, *40*, 2927–2931. [CrossRef]

20. Li, E.; Kakemoto, H.; Wada, S.; Tsurumi, T. Influence of CuO on the structure and piezoelectric properties of the alkaline niobate-based lead-free ceramics. *J. Am. Ceram. Soc.* **2007**, *90*, 1787–1791. [CrossRef]

21. Hagh, N.M.; Kerman, K.; Jadidian, B.; Safari, A. Dielectric and piezoelectric properties of Cu^{2+}-doped alkali niobates. *J. Eur. Ceram. Soc.* **2009**, *29*, 2325–2332. [CrossRef]

22. Zhao, Y.; Zhao, Y.; Huang, R.; Liu, R.; Zhou, H. Effect of sintering temperature on microstructure and electric properties of 0.95(K$_{0.5}$Na$_{0.5}$)NbO$_3$-0.05Li(Nb$_{0.5}$Sb$_{0.5}$)O$_3$ with copper oxide sintering aid. *J. Am. Ceram. Soc.* **2011**, *94*, 656–659. [CrossRef]

23. Yang, S.L.; Hong, C.S.; Tsai, C.C.; Liou, Y.C.; Chu, S.Y. Effects of modified-process on the microstructure, internal bias field, and activation energy in CuO-doped NKN ceramics. *J. Eur. Ceram. Soc.* **2012**, *32*, 1643–1650. [CrossRef]

24. Acker, J.; Kungl, H.; Hoffmann, M.J. Influence of Alkaline and Niobium Excess on Sintering and Microstructure of Sodium-Potassium Niobate (K$_{0.5}$Na$_{0.5}$)NbO$_3$. *J. Am. Ceram. Soc.* **2010**, *93*, 1270–1281. [CrossRef]

25. Ahn, C.W.; Nahm, S.; Karmarkar, M.; Viehland, D.; Kang, D.H.; Bae, K.S.; Priya, S. Effect of CuO and MnO$_2$ on sintering temperature, microstructure, and piezoelectric properties of 0.95(K$_{0.5}$Na$_{0.5}$)NbO$_3$-0.05BaTiO$_3$ ceramics. *Mater. Lett.* **2008**, *62*, 3594–3596. [CrossRef]

26. Perry, D.L. *Handbook of Inorganic Compounds*; CRC Press: Boca Raton, FL, USA, 2016.

27. Lin, D.; Kwok, K.W.; Chan, H. Piezoelectric and ferroelectric properties of Cu-doped K$_{0.5}$Na$_{0.5}$NbO$_3$ lead-free ceramics. *J. Phys. D Appl. Phys.* **2008**, *41*, 045401. [CrossRef]

28. Tan, X.; Fan, H.; Ke, S.; Zhou, L.; Mai, Y.W.; Huang, H. Structural dependence of piezoelectric, dielectric and ferroelectric properties of K$_{0.5}$Na$_{0.5}$(Nb$_{1-2x/5}$Cu$_x$)O$_3$ lead-free ceramics with high Q$_m$. *Mater. Res. Bull.* **2012**, *47*, 4472–4477. [CrossRef]

29. Lin, D.; Kwok, K.W.; Chan, H.L. Double hysteresis loop in Cu-doped K$_{0.5}$Na$_{0.5}$NbO$_3$ lead-free piezoelectric ceramics. *Appl. Phys. Lett* **2007**, *90*, 232903. [CrossRef]

30. Su, H.H.; Hong, C.S.; Tsai, C.C.; Chu, S.Y. Relaxor Behavior of Lead-Free Nonstoichiometric (Na$_{0.48-x}$K$_{0.48-x}$Li$_{0.04}$)Nb$_{0.89-x}$Ta$_{0.05}$Sb$_{0.06}$O$_3$-xSrTiO$_3$ Ceramics. *ECS J. Solid State Sci. Technol.* **2017**, *6*, N117. [CrossRef]

31. Hong, C.S.; Chu, S.Y.; Tsai, C.C.; Su, W.C.; Hsu, C.C. Effects of synthesized method on glassy behavior and freezing process of 0.75PFW-0.25PT ceramics. *J. Appl. Phys.* **2011**, *109*, 034106. [CrossRef]

32. Hong, C.S.; Chu, S.Y.; Su, W.C.; Chang, R.C.; Nien, H.H.; Juang, Y.D. The sintering temperature-induced transition from relaxor to ferroelectric in 0.7PbFe$_{2/3}$W$_{1/3}$O$_3$-0.3PbTiO$_3$ ceramics. *J. Alloys Compd.* **2008**, *459*, 1–7. [CrossRef]

33. Uchino, K. *Ferroelectric Devices*; CRC Press: Boca Raton, FL, USA, 2018.

34. Hench, L.L.; West, J.K. *Principles of Electronic Ceramics*, 1st ed.; Wiley-Interscience: Hoboken, NJ, USA, 1989.

35. Su, H.H.; Hong, C.S.; Tsai, C.C.; Chu, S.Y.; Lin, C.S. Effect of microstructure on the dielectric properties of (1-*x*)Na$_{0.5}$K$_{0.5}$NbO$_3$-*x*SrTiO$_3$ ceramics. *Ceram. Int.* **2016**, *42*, 17558–17564. [CrossRef]

36. Yang, Z.; Du, H.; Jin, L.; Hu, Q.; Qu, S.; Yang, Z.; Yu, Y.; Wei, X.; Xu, Z. A new family of sodium niobate-based dielectrics for electrical energy storage applications. *J. Eur. Ceram. Soc.* **2019**, *39*, 2899–2907. [CrossRef]

37. Liu, Q.; Zhu, F.Y.; Zhang, B.P.; Li, L.; Li, J.F. Dielectric and ferroelectric properties of AgSbO$_3$-modified (Li,K,Na)(Nb,Ta)O$_3$ lead-free piezoceramics. *J. Mater. Sci. Mater. Electron.* **2015**, *26*, 9309–9315. [CrossRef]